

Depth-Resolved Chemical Modification of Porous Silicon by Wavelength-Tuned Irradiation

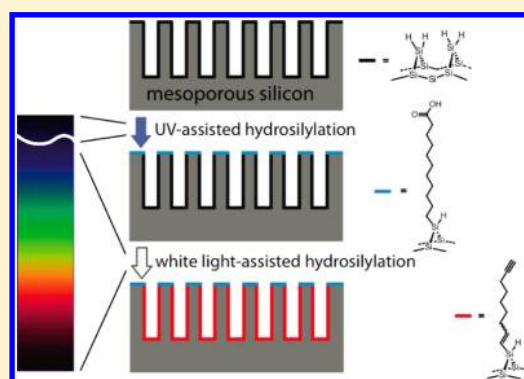
Bin Guan,[†] Simone Ciampi,[†] Erwann Luais,[†] Michael James,[§] Peter J. Reece,[‡] and J. Justin Gooding^{*,†}

[†]School of Chemistry and the Australian Centre for Nanomedicine and [‡]School of Physics, University of New South Wales, Sydney 2052, Australia

[§]Bragg Institute, Building 87, Australian Nuclear Science and Technology Organisation (ANSTO), Locked Bag 2001, Kirrawee DC 2232, Australia

Supporting Information

ABSTRACT: The ability to impart discrete surface chemistry to the inside and outside of mesoporous silicon is of great importance for a range of biomedical applications, from selective (bio)sensing to tissue-specific drug delivery. Here we present a generic strategy toward achieving depth-resolved functionalization of the external and internal porous surfaces by a simple change in the wavelength of the light being used to promote surface chemical reactions. UV-assisted hydrosilylation, limited by the penetration depth of UV light, is used to decorate the outside of the mesoporous structure with carboxylic acid molecules, and white light illumination triggers the attachment of dialkyne molecules to the inner porous matrix.



■ INTRODUCTION

Porous silicon (PSi) is a very promising material for optoelectronic and biological applications.¹ This is because of its optical properties,² tunable structure, and attractive surface reactivity.^{1,3,4} PSi with pore diameters in the 10–50 nm range (i.e., mesoporous silicon) has attracted interest for applications such as chemical and biological sensors⁵ and drug delivery.⁶ The ability to functionalize PSi surfaces precisely with self-assembled monolayers is critical for these applications.⁴ Surface reactions between organic molecules and freshly prepared PSi covered by silicon hydride species ensure protection from oxidative degradation and enable further introduction of distinct functional groups or biological species for sensing or delivery purposes. Moreover, it is necessary to develop surface modification strategies that allow for the introduction of different functionalities on the internal and external surfaces of PSi for the purposes of target-oriented sensing or localized drug delivery.⁷ For example, in a PSi device for targeted drug delivery in vivo, the exterior of the device must be decorated with biological recognition ligands for active targeting of the diseased sites whereas the inner pores could present chemistry compatible with the loading and release of specific drugs, imaging agents, or even nanoparticles for multistage drug release.⁸ Thus, active therapeutic agents could be guided to targeted organs or tissues without being exposed to complex biological matrices in vivo and could be released locally.

There have been a few reports on strategies to achieve bifunctionality on mesoporous silicon. Cunin and colleagues implemented the modified-etch idea.⁹ In their approach, flat silicon with covalently grafted organic layers on the surface was

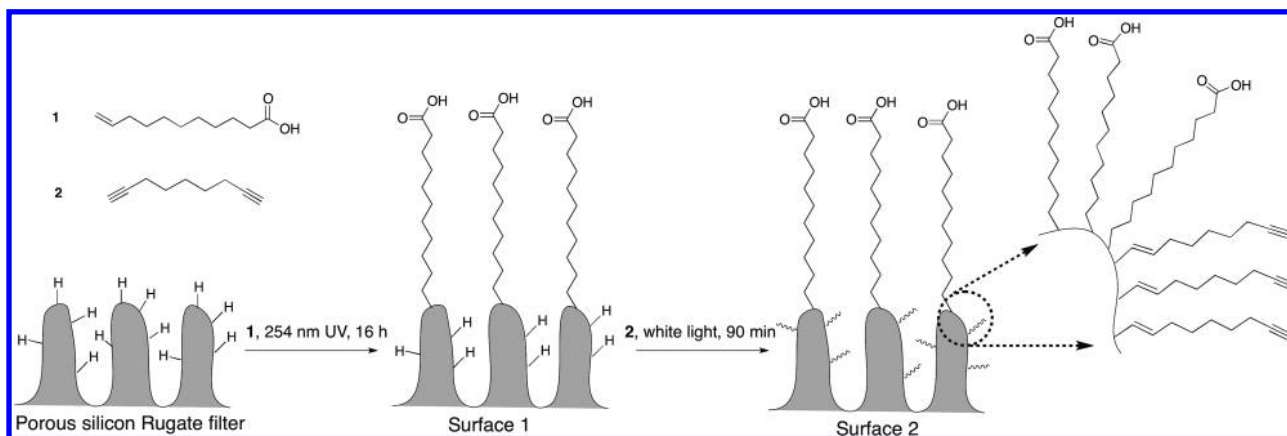
electrochemically etched. The resulting porous films featured an organic monolayer on the outer surface, leaving the fresh inner surface available for further modification. However, it is still uncertain as to how stable the organic monolayers on the surface were during the etching process. We have previously demonstrated an alternative approach based on the relative hydrophobicity of surface monolayers.¹⁰ Because water does not penetrate the hydrophobic mesopores, the exterior can be selectively modified in an aqueous solution. Upon wetting of the PSi interior with an organic solvent, different chemistry can be performed inside the pores. However, it was challenging to ensure the complete hydrophobicity of the pores. Recently, a chemical route via click chemistry was employed to provide different functionalities on acetylene-terminated mesoporous silicon.¹¹ By controlling the addition of the ligand in the click reaction, different functional groups were coupled to the inside and outside. Despite the success of the previous two chemical routes, both require fine tuning of the pore dimension. A more generic approach to achieving discrete derivatization of the PSi surfaces for target-oriented applications is therefore highly desirable.

In this context, both UV- and visible light-induced modification of silicon using either 1-alkenes or 1-alkynes has been reported as an effective approach toward the formation of Si–C bonds, yielding densely packed and stable molecular films.^{12,13} Because the absorption depth of light through the

Received: September 11, 2012

Revised: October 14, 2012

Published: October 18, 2012

Scheme 1. Depth-Resolved Hydrosilylation of Mesoporous Silicon with Bifunctional Surface Molecules^a

^aFreshly prepared PSi was reacted with acid 1 at room temperature under illumination with 254 nm UV light for 16 h (surface 1). The unaltered internal silicon hydride groups on surface 1 were subsequently functionalized with diyne 2 by visible light illumination for 90 min (surface 2).

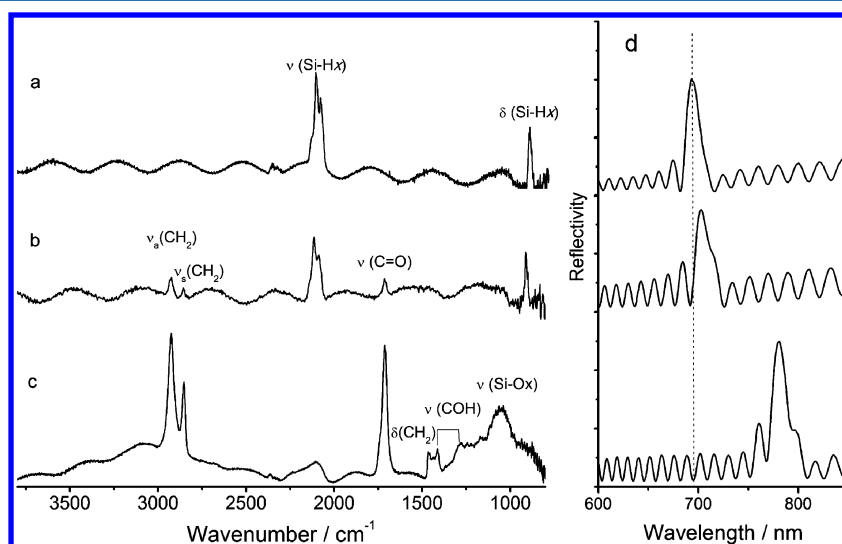


Figure 1. Transmission FTIR spectra of PSi rugate filters passivated with undecylenic acid 1: (a) a freshly etched PSi surface, (b) after 16 h of UV reaction, (c) after thermal hydrosilylation, and (d) their corresponding optical reflectivity spectra showing the optical shifts caused by the acid molecules grafting onto the PSi surfaces.

porous structure is a strong function of wavelength, changes in the wavelength of light could lead to depth-resolved surface functionalization. In this letter, we explore the ability of UV and visible light to promote distinct surface modifications on the interior and exterior of mesoporous silicon, respectively. PSi rugate filters, a class of photonic band gap structures with a sinusoidal refractive index profile,¹⁴ are employed to demonstrate this strategy. As depicted in Scheme 1, a monolayer of undecylenic acid (1) was formed on the external surfaces of freshly prepared PSi rugate filters upon irradiation for 16 h with 254 nm UV light (surface 1). Internal silicon hydride groups left unreacted on surface 1 were subsequently functionalized with 1,8-nonadiyne (2) by visible-light illumination for 90 min at room temperature, yielding two types of surface chemistry at two different depths of the mesoporous material (surface 2) (i.e., carboxyls on the exterior and acetylenes on the interior). The two typical surface molecules were chosen for this proof-of-principle study because both functionalities are well suited for further surface modifications.^{15,16}

EXPERIMENTAL SECTION

Fabrication of PSi Rugate Filters. Mesoporous silicon rugate filters with 40 sinusoidally varying refractive index layers, a porosity variation of 54.5 to 57.5%, and an average pore size of ca. 20 nm were prepared by the anodization of Si(100) substrates in a 25% (v/v) hydrofluoric acid ethanolic solution at room temperature, as described previously.¹¹ The thickness of the PSi structure is ca. 10 μm as determined by scanning electron microscopy. After anodization, the samples were rinsed in ethanol, dried under nitrogen gas, and stored under dry argon prior to analysis or further reaction.

UV-Mediated Hydrosilylation. PSi rugate filter samples and Si(100) samples were immersed in neat deoxygenated 1 (Sigma-Aldrich, >98%) and were reacted under the irradiation of a 254 nm UV lamp (1.8 mW/cm^2) in an inert nitrogen atmosphere for 16 h. The samples were then rinsed with copious dichloromethane and ethanol and dried with argon gas. Control experiments under thermal conditions for the hydrosilylation of undecylenic acid on Si(100) and PSi samples were performed according to a previous report.¹⁷

White-Light-Induced Hydrosilylation on Bulk PSi. PSi rugate filters were immersed in deoxygenated 2 (Alfa Aesar, 98%) in a Schlenk vessel under an argon atmosphere. A high-intensity-fiber white-light source (150 W halogen lamp) was used to illuminate the PSi sample. To reduce thermal effects, an infrared filter was fitted

between the light source and the PSi samples. After 90 min of illumination, the PSi films were cleaned with a copious amount of dichloromethane and ethanol and dried under argon for further analysis. A control experiment of thermal hydrosilylation with diyne 2 on PSi was also conducted as reported previously.¹⁸

Surface Characterization. Optical reflectivity spectra of PSi films were recorded in the visible and near-infrared at normal incidence using a custom-built optical arrangement. The setup incorporated an Ocean Optics USB2000+ miniature fiber optic spectrometer and a fiber-coupled halogen light source. The recorded spectra have a resolution of 1 nm, and the measurement spot size was approximately 100 μm . Fourier transfer infrared (FTIR) spectra of PSi rugate filters were obtained in transmission mode on a ThermoNicolet Avatar 370-FTIR spectrometer, relative to unmodified Si(100), by selecting a 4 cm^{-1} resolution and accumulating a minimum of 128 scans. X-ray photoelectron spectroscopy (XPS) was carried out on an Escalab 220iXL spectrometer with a monochromated Al K α source (1486.6 eV) incident at 58° to a hemispherical analyzer, and a multichannel detector at a takeoff angle of 90° from the plane of the sample surface. The depth profiling was studied by recording spectra between Ar sputtering steps. During the sputtering, Ar flowed through the ion gun, increasing the working pressure to $\sim 5 \times 10^{-7}$ Torr, and the voltage on the ion gun was set to 5 kV. X-ray reflectivity (XRR) profiles were measured under ambient conditions (30 °C and 35% relative humidity) on a Panalytical Ltd X'Pert Pro reflectometer using Cu K α X-ray radiation ($\lambda = 1.54056$ Å). The X-ray beam was collimated using a Göbel mirror with a 0.1 mm slit and a post sample beam collimator. To minimize the effects of nanoscale water condensation on these surfaces, measurements were started approximately 10 min after exposing the samples to air.¹⁹ Reflectivity data were collected over the angular range of $0.05^\circ \leq \theta \leq 5.00^\circ$ in steps of 0.010° and counting 10 s per step. Structural parameters of the measured films were refined using the MOTOFIT analysis software and the Levenberg–Marquardt method to minimize χ^2 values of the fits.²⁰ Reflectivity data are presented as a function of the momentum transfer vector normal to the surface $Q = 4\pi(\sin \theta)/\lambda$.

RESULTS AND DISCUSSION

UV-Induced Hydrosilylation on PSi Rugate Filters and Flat Si(100). Figure 1a shows a typical transmission FTIR spectrum of freshly etched PSi with Si–H $_x$ ($x = 1, 2, 3$) stretching and bending modes at ~ 2100 and ~ 900 cm^{-1} , respectively. UV-assisted hydrosilylation with acid species 1 affords surface 1 (Scheme 1). The appearance of asymmetrical and symmetrical stretching modes of methylene units at 2930 and 2850 cm^{-1} and the carbonyl stretching at 1700 cm^{-1} from the carboxylic acid (Figure 1b) confirms the formation of an acid layer on the PSi surface. Compared to the spectrum of a completely passivated PSi sample by thermal hydrosilylation²¹ (Figure 1c), the partial attenuation of Si–H $_x$ modes suggests that the majority of the PSi bulk structure remains unmodified. The optical reflectivity measurements displayed in Figure 1d, unique to PSi rugate samples, indicate a measurable change in the material refractive index. A ca. 10 nm shift toward longer wavelengths (the so-called red shift) was detected upon UV modification, a significantly smaller shift when compared to the ca. 57 nm red shift accompanying the complete passivation of the PSi matrix via the thermal method. The latter value is comparable to previous studies of PSi rugate filters functionalized with undecylenic acid.¹⁷ Our data for the UV method suggest partial monolayer coverage for the PSi structure using 16 h of UV reactions. We hypothesize that this partial monolayer is in fact on the exterior surface of the PSi, plus a small amount of modification near the entrance to the pores.

Flat hydride-terminated Si(100) surfaces were also modified with undecylenic acid using UV-assisted hydrosilylation to

verify the formation of high-density self-assembled monolayers using UV light. XPS analysis demonstrates the monolayer formation (Figure S1 in the Supporting Information). Importantly, no significant silicon oxide or suboxide silicon was detected in 102–104 eV region of the high-resolution Si spectrum, indicating the formation of an acid monolayer without oxidation on the surface.²² Furthermore, X-ray reflectivity profiles of the modified Si(100) were measured to gain further structural information (Figure 2) on the acid film.

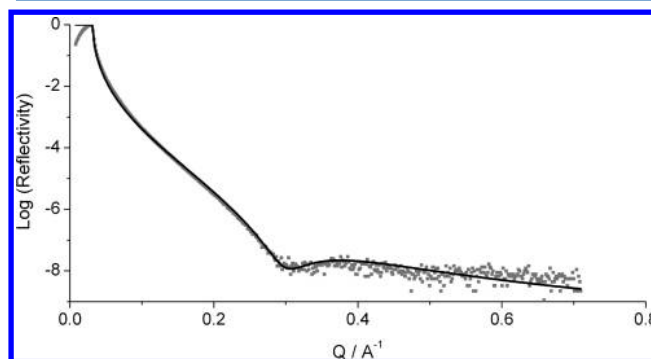


Figure 2. Observed X-ray reflectometry spectrum (data points) acquired on an undecylenic acid-functionalized Si(100) surface after 16 h of UV irradiation. The solid line is the calculated reflectivity profile based on the refined structural model.

The refined thickness of the monolayer was found to be 9.9 Å with an electron density of $0.28 \text{ e}^- \text{ Å}^{-3}$. Comparison with the literature value of 9–11 Å for an undecylenic acid monolayer²³ indicates a well-formed, densely packed monolayer effectively passivating the underlying silicon substrates. Therefore, it is suggested that the unaltered silicon hydride groups observed in the FTIR spectra of the UV-irradiated PSi sample (Figure 1b) are predominantly from the internal surface with the exterior surface modified by a monolayer of undecylenic acid.

XPS Depth Profiling on UV-Modified PSi. How light propagates through an optical medium can be described by the penetration depth at which the intensity of the radiation inside the material retains $1/e$ (about 37%) of its original value at the surface. As reported in the literature, the penetration depth of UV light can reach several to hundreds of nanometers into a PSi structure, depending on the wavelength of light and the porosity of the material.²⁴ For a PSi rugate filter with 54.5–57.5% porosity, the penetration depth of 254 nm UV light is calculated to be less than 50 nm.²⁵ Hence, it is assumed that UV-mediated modification occurs mainly on the top 50 nm of PSi surfaces. To verify that there was some modification near the pore entrances when UV light was used to form the monolayer, XPS depth profiling with argon ion sputtering was employed. This technique is physically able to remove materials from the surface by ion bombardment while in situ XPS data of the surface are collected. The removal effect was confirmed by atomic force microscopy and scanning electron microscopy on the PSi samples after ion sputtering (Figures S3 and S4 in the Supporting Information).

Flat Si(100) functionalized under UV irradiation was first examined in order to establish a baseline for the rate of ion sputtering on silicon. Thereafter, PSi samples that reacted for 16 h under UV irradiation with acid molecule 1 were analyzed by XPS ion sputtering and compared with thermally modified positive control PSi samples (i.e., samples where a full monolayer is formed on both the interior and exterior surfaces).

Survey and high-resolution scans were collected (comparable to those shown in Figures S1 and S2 in the Supporting Information) at time intervals during the sputtering process. The XPS-derived carbon 1s content, plotted as a function of sputtering time, is presented in Figure 3. As the inset graph

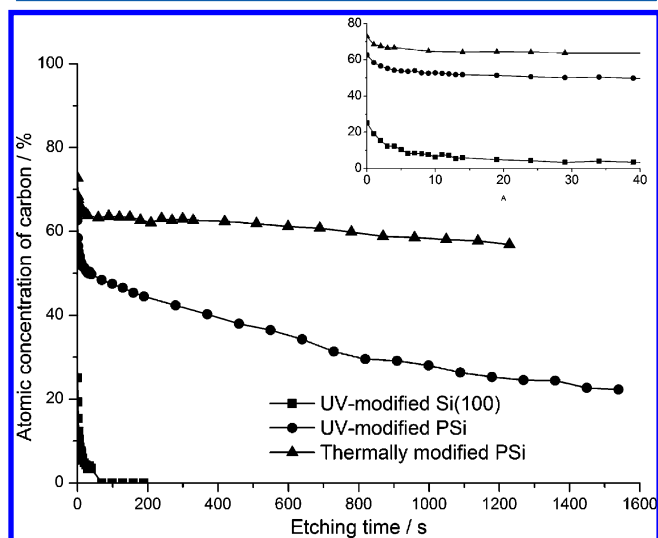


Figure 3. XPS depth profiling of acid monolayers on flat Si(100) and PSi surfaces: atomic concentration of carbon from C 1s high-resolution scans as a function of the argon ion etching time. The inset graph shows the change in carbon atomic content in the first 40 s of sputtering.

displays, the total amount of carbon on flat Si(100) surfaces modified with acid **1** drops dramatically within the first 20 s of sputtering time, indicating the removal of acid molecules from the densely packed monolayer by argon ion etching. After 40 s, no carbon signal can be detected on flat Si(100) samples, suggesting the complete removal of the monolayer from the sample surface. The monolayer thickness on flat silicon is about 1 nm based on X-ray reflectivity measurements; therefore, the argon-ion-sputtering-induced removal of the organic layer was estimated to occur at a rate of approximately 0.25 Å/s. In contrast, UV-modified PSi surfaces show a substantially slower decrease in carbon content upon argon ion bombardment. After etching was carried out for 26 min (1560 s, corresponding to an etching depth of ca. 39 nm), the total amount of carbon from the UV-modified PSi surface fell to 35.6% (approximately $1/e$) of its original value. This decrease in carbon content to $1/e$ approximates to the definition of the penetration depth, (i.e., the UV penetration depth for the PSi rugate filter is ca. 39 nm), which supports the hypothesis that UV radiation and hence the hydrosilylation reaction are concentrated within the first 50 nm of the 10- μ m-thick PSi structure. In contrast, thermally modified PSi with a full coverage of monolayer on both the exterior and interior displays a much higher initial carbon atomic concentration and a much slower decline in carbon content with sputtering time, in comparison to the case of PSi samples functionalized under UV conditions. The UV-assisted functionalization of PSi occurring principally on the top 50 nm of the PSi structure (including exterior and adjacent pore areas) is consistent with FTIR and reflectivity data, and it can be concluded that UV-assisted hydrosilylation reactions yield a dense monolayer on the exterior surface of the PSi with some

degree of modification occurring within the uppermost 50 nm of the PSi film.

White-Light-Induced Hydrosilylation on PSi. Although UV radiation leads to the preferential modification of the external surfaces on PSi, visible light, which can penetrate into the pores, was utilized to passivate the entire surfaces of the PSi rugate filters. Figure 4 displays the XPS results from a PSi

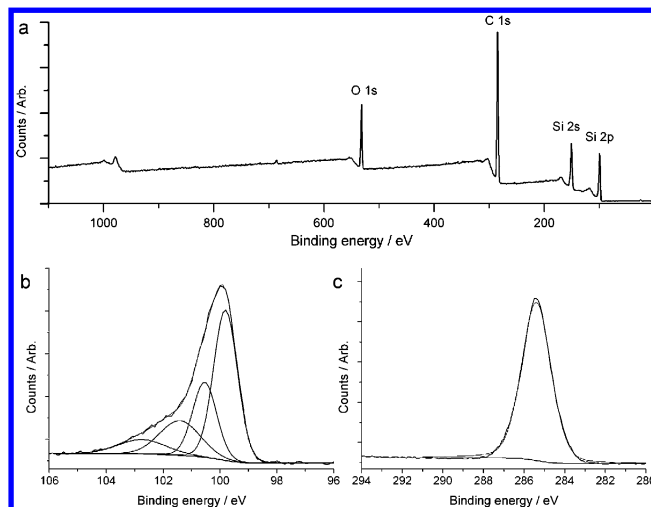


Figure 4. XPS analysis of acetylene-terminated alkyne monolayers on a PSi rugate filter after white-light illumination in diyne **2** for 90 min: (a) survey scan, (b) high-resolution scan of the Si 2p region, and (c) C 1s narrow scan.

rugate filter after reacting with diyne **2** for 90 min under visible-light illumination. A representative survey spectrum in Figure 4a shows the presence of Si, C, and O only. High-resolution narrow scans were collected for the C 1s and Si 2p regions to obtain information on bonding configurations and on the presence of any oxidation of the silicon substrate. The narrow scan of Si 2p (Figure 4b) shows a clear Si 2p_{1/2}–Si 2p_{3/2} spin-orbit-split doublet (99.9 and 99.3 eV, respectively) from bulk silicon. In the 102–104 eV region, silicon oxide or suboxide was detected, indicating some degree of oxidation during hydrosilylation. This result agrees with the increase in the Si–O stretching mode at 1100 cm^{−1} in the transmission FTIR spectrum of the sample (Supporting Information, Figure S5). The growth of oxides on the surfaces might be explained by one of the possible mechanisms of white-light hydrosilylation: a trace amount of molecular oxygen in the reaction chamber initiated the radical chain reaction for hydrosilylation.²⁶ The narrow C 1s scan (Figure 4c) reveals a broad peak at 285 eV corresponding to aliphatic carbon-bonded carbon from alkyne molecules, which verifies the formation of an alkyne monolayer. In addition, the FTIR spectra (Supporting Information, Figure S5) with $\nu(\text{C}\equiv\text{CH})$, $\nu_{\text{a}}(\text{CH}_2)$, $\nu_{\text{s}}(\text{CH}_2)$, $\nu(\text{SiC}\equiv\text{C})$, and $\delta(\text{CH}_2)$ modes at 3310, 2932, 2848, 1595, and 1440 cm^{−1}, respectively, and the decrease in the stretching and bending signals of Si–H_x ($x = 1, 2, 3$) further confirm the formation of a Si–C-bound alkyne monolayer. Derivatized PSi is also characterized by optical reflectivity measurements (Supporting Information, Table S1). It is demonstrated that the optical shift resulting from light-promoted functionalization is comparable to that of the thermal modification with a sufficient coverage of molecules to confer high stability to PSi in the aqueous solution, as we have demonstrated previously.^{11,18} Moreover,

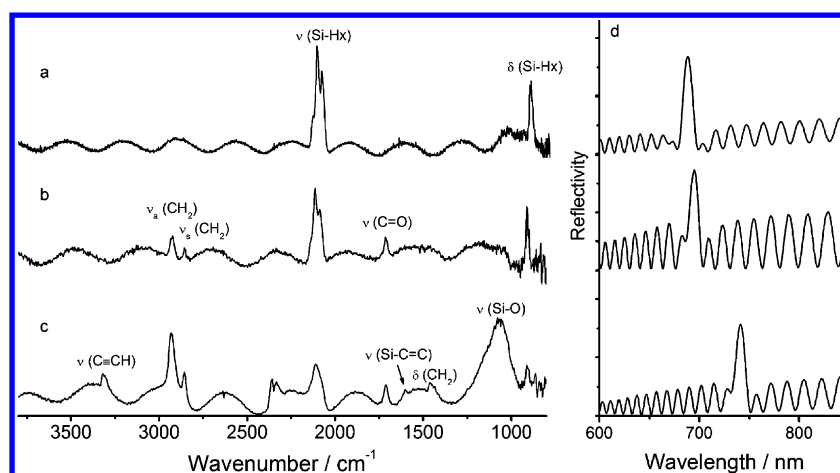


Figure 5. Transmission FTIR spectra of (a) freshly prepared PSi, (b) the rugate filter after UV-assisted hydrosilylation with acid species **1** on the exterior of the PSi (surface 1), and (c) bifunctionalized PSi where visible light is used to modify the interior of PSi (surface 2). (d) Optical reflectivity spectra of the three surfaces.

the optical shift caused by monolayer formation upon white-light illumination for 90 min is 61.3 ± 3.2 nm, in agreement with the theoretical value (58.9 nm) calculated from the refractive index contrast of PSi before and after complete modification.²⁷ Therefore, white-light hydrosilylation is capable of functionalizing the entire PSi surface efficiently.

Bifunctional Modification of PSi. As proposed in Scheme 1, bifunctional PSi with a carboxyl-terminated exterior and an acetylene-terminated interior can be achieved. Each step in the functionalization was monitored by FTIR and optical reflectivity techniques (Figure 5).

As shown in Figure 5b, the presence of asymmetrical and symmetrical stretching of CH_2 at 2930 and 2850 cm^{-1} , CH_2 bending at 1440 cm^{-1} , and $\text{C}=\text{O}$ stretching at 1700 cm^{-1} verifies surface 1 after 16 h of reaction with **1** under UV irradiation. The fact that the Si-H_x peaks remain distinct in Figure 5b and only a slight shift toward longer wavelength is observed in the middle spectrum of Figure 5d agrees with the presence of unaltered pore areas for surface 1. White-light-induced hydrosilylation with diyne **2** on surface 1 yields surface 2. The corresponding FTIR spectrum for surface 2 is displayed in Figure 5c. The appearance of $\nu(\text{C}\equiv\text{CH})$ at 3310 cm^{-1} and $\nu(\text{Si-C}\equiv\text{C})$ at 1595 cm^{-1} and the increase in CH_2 stretching support the formation of an alkyne monolayer on the internal surface. Moreover, a small but distinct peak at 1720 cm^{-1} for $\nu(\text{C}=\text{O})$ derived from acid species **1** on the external areas again provides evidence for a bifunctional PSi surface (surface 2). The corresponding optical reflectivity spectrum for the bifunctional surface (Figure 5d) reveals a ca. 50 nm optical shift caused by the alkyne molecule **2** in the pores of the PSi rugate filter and is consistent with the above FTIR results.

CONCLUSIONS

We have demonstrated a generic and flexible approach to introducing different functional groups on the external and internal surfaces of mesoporous silicon on the basis of wavelength-tuned light irradiation. UV-promoted hydrosilylation decorates only the external surface and its adjacent pore area of PSi. White-light hydrosilylation is able to modify the entire pore surface of PSi and provides a simple and efficient method of surface modification. A bifunctional PSi film with a carboxyl-terminated exterior and an acetylene-terminated

interior was successfully achieved by physically tuning the wavelength of radiation light for hydrosilylation.

On the basis of recent publications on the photochemical grafting of organic monolayers on semiconductor materials,^{28–30} this approach could also potentially be applicable to other porous materials, such as porous TiO_2 , ZnO , and indium tin oxide. Because they all show sufficient absorption in the UV and transparency in the visible region, by carefully changing the wavelength of radiation, we could also achieve depth-resolved modification on those porous materials.

ASSOCIATED CONTENT

Supporting Information

Additional experimental data. X-ray photoelectron spectroscopy (XPS) data on both $\text{Si}(100)$ and PSi surfaces. XPS depth profiling result on unmodified PSi. Atomic force microscopy (AFM), scanning electronic microscopy (SEM), and epi-illumination images of PSi before and after ion sputtering. FTIR spectra and optical reflectivity data of PSi rugate filters having undergone a white-light-promoted reaction. Penetration depth profile of PSi. This material is available free of charge via the Internet at <http://pubs.acs.org>.

AUTHOR INFORMATION

Corresponding Author

*E-mail: justin.gooding@unsw.edu.au.

Notes

The authors declare no competing financial interest.

ACKNOWLEDGMENTS

The authors thank the Australian Research Council (DP110902183) and the National Health and Medical Research Council (APP1024723) for support. We thank Dr. Bill Bin Gong (Mark Wainwright Analytical Center, University of New South Wales) for his assistance with XPS depth profiling, Dr. Guillaume Le Saux (School of Chemistry, University of New South Wales) for help with XPS and AFM, and Mr. Craig Johnson (School of Physics, University of New South Wales) for calculating the theoretical penetration depth.

REFERENCES

- (1) Stewart, M. P.; Buriak, J. M. Chemical and biological applications of porous silicon technology. *Adv. Mater.* **2000**, *12*, 859–869.
- (2) Theiss, W. Optical properties of porous silicon. *Surf. Sci. Rep.* **1997**, *29*, 91–192.
- (3) Lehmann, V.; Stengl, R.; Luigart, A. On the morphology and the electrochemical formation mechanism of mesoporous silicon. *Mater. Sci. Eng. B* **2000**, *69–70*, 11–22.
- (4) Kilian, K.; Böcking, T.; Gooding, J. The importance of surface chemistry in mesoporous materials: lessons from porous silicon biosensors. *Chem. Commun.* **2009**, 630–640.
- (5) Jane, A.; Dronov, R.; Hodges, A.; Voelcker, N. H. Porous silicon biosensors on the advance. *Trends Biotechnol.* **2009**, *27*, 230–239.
- (6) Prestidge, C. A.; Barnes, T. J.; Lau, C.-H.; Barnett, C.; Loni, A.; Canham, L. Mesoporous silicon: a platform for the delivery of therapeutics. *Expert Opin. Drug Delivery* **2007**, *4*, 101–110.
- (7) Kilian, K. A.; Lai, L. M. H.; Magenau, A.; Cartland, S.; Böcking, T.; Di Girolamo, N.; Gal, M.; Gaus, K.; Gooding, J. J. Smart tissue culture: in situ monitoring of the activity of protease enzymes secreted from live cells using nanostructured photonic crystals. *Nano Lett.* **2009**, *9*, 2021–2025.
- (8) Mann, A. P.; Tanaka, T.; Somasunderam, A.; Liu, X.; Gorenstein, D. G.; Ferrari, M. E-selectin-targeted porous silicon particle for nanoparticle delivery to the bone marrow. *Adv. Mater.* **2011**, *23*, H278–H282.
- (9) Pace, S.; Gazagnes, L.; Gonzalez, P.; Guimon, C.; Granier, M.; Cot, D.; Devoisselle, J.-M.; Cunin, F. New approach for the selective chemical functionalization of porous silicon films with organic monolayers. *Phys. Status Solidi A* **2009**, *206*, 1326–1329.
- (10) Kilian, K. A.; Böcking, T.; Gaus, K.; Gooding, J. J. Introducing distinctly different chemical functionalities onto the internal and external surfaces of mesoporous materials. *Angew. Chem., Int. Ed.* **2008**, *47*, 2697–2699.
- (11) Guan, B.; Ciampi, S.; Le Saux, G.; Gaus, K.; Reece, P. J.; Gooding, J. J. Different functionalization of the internal and external surfaces in mesoporous materials for biosensing applications using “click” chemistry. *Langmuir* **2011**, *27*, 328–334.
- (12) Terry, J.; Linford, M. R.; Wigren, C.; Cao, R.; Pianetta, P.; Chidsey, C. E. D. Determination of the bonding of alkyl monolayers to the Si(111) surface using chemical-shift, scanned-energy photoelectron diffraction. *Appl. Phys. Lett.* **1997**, *71*, 1056–1058.
- (13) Stewart, M. P.; Buriak, J. M. Photopatterned hydrosilylation on porous silicon. *Angew. Chem., Int. Ed.* **1998**, *37*, 3257–3260.
- (14) Bovard, B. G. Rugate filter theory: an overview. *Appl. Opt.* **1993**, *32*, 5427–5442.
- (15) Hermanson, G. T. *Bioconjugate Techniques*, 2nd ed.; Academic Press: Boston, 2008; Chapter 3, pp 213–233.
- (16) Kolb, H. C.; Finn, M. G.; Sharpless, K. B. Click chemistry: diverse chemical function from a few good reactions. *Angew. Chem., Int. Ed.* **2001**, *40*, 2004–2021.
- (17) Kilian, K. A.; Böcking, T.; Ilyas, S.; Gaus, K.; Jessup, W.; Gal, M.; Gooding, J. J. Forming antifouling organic multilayers on porous silicon rugate filters towards in vivo/ex vivo biophotonic devices. *Adv. Funct. Mater.* **2007**, *17*, 2884–2890.
- (18) Ciampi, S.; Böcking, T.; Kilian, K. A.; Harper, J. B.; Gooding, J. J. Click chemistry in mesoporous materials: functionalization of porous silicon rugate filters. *Langmuir* **2008**, *24*, 5888–5892.
- (19) James, M.; Darwish, T. A.; Ciampi, S.; Sylvester, S. O.; Zhang, Z.; Ng, A.; Gooding, J. J.; Hanley, T. L. Nanoscale condensation of water on self-assembled monolayers. *Soft Matter* **2011**, *7*, 5309–5318.
- (20) Nelson, A. Co-refinement of multiple-contrast neutron/X-ray reflectivity data using MOTOFIT. *J. Appl. Crystallogr.* **2006**, *39*, 273–276.
- (21) Boukherroub, R.; Wojtyk, J. T. C.; Wayner, D. D. M.; Lockwood, D. J. Thermal hydrosilylation of undecylenic acid with porous silicon. *J. Electrochem. Soc.* **2002**, *149*, H59–H63.
- (22) Cerofolini, G. F.; Galati, C.; Renna, L. Accounting for anomalous oxidation states of silicon at the Si/SiO₂ interface. *Surf. Interface Anal.* **2002**, *33*, 583–590.
- (23) Böcking, T.; Wong, E. L. S.; James, M.; Watson, J. A.; Brown, C. L.; Chilcott, T. C.; Barrow, K. D.; Coster, H. G. L. Immobilization of dendrimers on Si-C linked carboxylic acid-terminated monolayers on silicon(111). *Thin Solid Films* **2006**, *515*, 1857–1863.
- (24) Fox, M. *Optical Properties of Solids*; Oxford University Press: New York, 2010; Vol. 3, p 58.
- (25) According to Beer–Lambert’s law in which the intensity of light inside a material decays exponentially from the surface, the penetration depth at which the intensity falls to $1/e$ of its surface value is the reciprocal of the adsorption coefficient. The adsorption coefficient is proportional to the imaginary part of the complex refractive index of the light medium—PSi (which is then determined by the porosity based on the Bruggeman model)—and inversely proportional to the wavelength of light. Hence, the penetration depth of 254 nm UV light to ca. 56% porosity of the PSi rugate structure can be calculated. The correlation between the penetration depth for PSi used in this study and the wavelength is shown in the Supporting Information (Figure S6).
- (26) Liu, Y.; Yamazaki, S.; Yamabe, S.; Nakato, Y. A mild and efficient Si (111) surface modification via hydrosilylation of activated alkynes. *J. Mater. Chem.* **2005**, *15*, 4906–4913.
- (27) On the basis of the theory of rugate filter, the optical shift ($\Delta\lambda$) caused by surface modification is related to the change in refractive index (Δn), the initial refractive index of PSi (n_0), and the peak position in the spectrum (λ_0), which can be described by $\Delta\lambda/\lambda_0 = \Delta n/n_0$. The refractive index of PSi is estimated according to Looyenga effective medium theory (Looyenga, H. Dielectric constants of heterogeneous mixtures. *Physica* **1965**, *31*, 401–406). With a full monolayer of 1,8-nonadiyne with a refractive index of 1.45 formed on the surfaces of the PSi rugate filter, the corresponding optical shift is calculated to be 58.9 nm.
- (28) Li, Y.; Zuilhof, H. Photochemical grafting and patterning of organic monolayers on indium tin oxide substrates. *Langmuir* **2012**, *28*, 5350–5359.
- (29) Franking, R.; Kim, H.; Chambers, S. A.; Mangham, A. N.; Hamers, R. J. Photochemical grafting of organic alkenes to single-crystal TiO₂ surfaces: a mechanistic study. *Langmuir* **2012**, *28*, 12085–12093.
- (30) Li, Y.; Zhao, M.; Wang, J.; Liu, K.; Cai, C. Biofunctionalization of a “clickable” organic layer photochemically grafted on titanium substrates. *Langmuir* **2011**, *27*, 4848–4856.